HHS Public Access

Author manuscript

Science. Author manuscript; available in PMC 2015 July 29.

Published in final edited form as:

Science. 2014 August 29; 345(6200): 1058–1062. doi:10.1126/science.1257861.

Dynamic signaling by T follicular helper cells during germinal center B cell selection

Ziv Shulman[1], **Alexander D. Gitlin**[1], **Jason S. Weinstein**[2], **Begoña Lainez**[2,3], **Enric Esplugues**[3,4], **Richard A. Flavell**[4,5], **Joseph E. Craft**[2,4], and **Michel C. Nussenzweig**[1,5]

[1]Laboratory of Molecular Immunology, The Rockefeller University; New York, New York 10065; USA

[2]Department of Internal Medicine (Rheumatology), Yale University School of Medicine, New Haven, CT 06520; USA

[4]Department of Immunobiology, Yale University School of Medicine, New Haven, CT 06520; USA

[5]Howard Hughes Medical Institute, The Rockefeller University; New York, New York 10065; USA

Abstract

T follicular helper (T_{FH}) cells select high-affinity, antibody-producing B cells for clonal expansion in germinal centers (GCs), but the nature of their interaction is not well defined. Using intravital imaging, we found that selection is mediated by large but transient contacts between T_{FH} and GC B cells presenting the highest levels of cognate peptide bound to major histocompatibility complex II. These interactions elicited transient and sustained increases in T_{FH} intracellular free calcium (Ca^{2+}) that were associated with T_{FH} cell coexpression of the cytokines interleukin-4 and -21. However, increased intracellular Ca^{2+} did not arrest T_{FH} cell migration. Instead, T_{FH} cells remained motile and continually scanned the surface of many GC B cells, forming short-lived contacts that induced selection through further repeated transient elevations in intracellular Ca^{2+}.

Germinal centers (GCs) are specialized microanatomical sites where B cells undergo clonal expansion, somatic hypermutation, and affinity maturation (1–3). Through iterative cycles of diversification and selection, the GC produces high-affinity memory B and plasma cells (2–4). Selection of high-affinity GC B cells requires their interaction with T follicular helper (T_{FH}) cells, which must discern among B cell clones according to their surface density of peptide–major histocompatibility complex II (pMHCII) (5). GC B cells are then programmed by T_{FH} cells to expand and hypermutate in direct proportion to the levels of cognate antigen presented(6). These events are controlled by T_{FH} cell–derived signals, including membrane-bound inducible costimulator (ICOS) and CD40L and the cytokines

Address correspondence to: Michel C. Nussenzweig, Laboratory of Molecular Immunology, Rockefeller University, 1230 York Avenue, New York, NY, 10065, nussen@rockefeller.edu.

[3]Present Address: Immunology Institute, Department of Medicine, Icahn School of Medicine at Mount Sinai, New York, New York, USA.

Supplementary Materials:
Materials and Methods
Supplementary References
Figures S1-S8
Capitations for Movies S1 to S12

interleukin-4 (IL-4) and IL-21 (7, 8), which are delivered in short-lived intercellular contacts (9).

To examine how the interactions between T_{FH} cells and GC B cells control selection, we imaged cells expressing genetically encoded fluorescent proteins in vivo by means of two-photon laser scanning microscopy (TPLSM). Ovalbumin (OVA)–specific, T cell receptor (TCR) transgenic OT-II T cells expressing DsRed were adoptively transferred into congenic mice before priming with OVA in alum. After 2 to 3 weeks, a 95:5 mixture of non fluorescent *Ly75*$^{-/-}$ and GFP^{+} *Ly75*$^{-/-}$ (*Ly75* encodes the cell-surface receptor DEC205) B cells, both specific for NP (4-hydroxy-3-nitrophenylacetyl; B1-8^{hi}) (10), was transferred before boosting with soluble OVA conjugated to NP (NP–OVA) (11, 12). To induce selection, we increased the levels of pMHCII on the surface of GC B cells 7 to 8 days later through injection of DEC205 antibody fused to the cognate antigen OVA (αDEC-OVA) (Fig. 1A). This chimeric antibody targets DEC205, an endocytic receptor that carries associated proteins into MHCII-processing compartments of GC B cells (5). As a result, targeted GC B cells are initially retained in the GC light zone (LZ) and thereafter proliferate in the dark zone (DZ) (5, 6). As a control, mice were injected with chimeric DEC205 antibody fused to an irrelevant antigen (*Plasmodium falciparum* circumsporozoite protein, αDEC-CS)(5). Popliteal lymph nodes were exposed after 4 to 10 hours, GCs were imaged by means of TPLSM (Fig. 1A), and the results were subjected to colocalization analysis (fig. S1).

Consistent with previous observations (9, 11, 13–16), GC lymphocytes were highly motile (T_{FH} cells, 9 μm/min and B cells, 6.6 μm/min) (Fig. 1, B and C, and movie S1). Under steady-state conditions, in which an unknown fraction of B cells are being positively selected, the majority of T-B contacts were short-lived (Fig. 1, B and D, and movie S1). Positive selection through αDEC-OVA injection was associated with a reduction in both GC B and T_{FH} cell velocities, along with an increase in the duration of the T-B contacts ($P < 0.0001$) (Fig. 1, B to D, and movies S2 and S3). In particular, the fraction of conjugates lasting 5 min or longer increased from 2.7 to 20.7% of the total interactions (Fig. 1D), and these occasionally moved at the B cell velocity (4.16 μm/min on average) (Fig. 1E). Although most of the conjugates moved short distances, and it was not possible to determine which one of the partners drags the other (movie S2), in those cases that could be interpreted the conjugates were led by the B cell and rarely, if at all, by the T cell (movie S3). Thus, even under conditions of enforced selection, most T-B interactions resembled those found under physiologic conditions in that they remained transient, with T cells forming and breaking contacts with multiple B cells (Fig. 1D and movie S3). Volume analysis of the T-B colocalized area revealed that the average contact size of the stable T-B conjugates (>5 min) was enlarged threefold during positive selection compared with control (Fig. 1F). As expected, polyclonal follicular B cells within the mantle zone did not slow down or form contacts with T_{FH} cells after αDEC-OVA injection (fig. S2 and movie S4). We conclude that positive selection through increased pMHCII on GC B cells is associated with longer but dynamic T-B contacts involving a larger surface area between the two interacting cells.

To examine whether positive selection interferes with the interactions between T_{FH} cells and GC B cells presenting low levels of pMHCII, we directly imaged selected and nonselected B

cells within the same GC. GCs containing OT-II DsRed$^+$ T cells and a mixture of B1-8^{hi} GFP$^+$ *Ly75*$^{-/-}$, CFP$^+$ *Ly75*$^{+/+}$, and nonfluorescent *Ly75*$^{-/-}$ B cells at a ~5:5:90 ratio were generated and imaged as in Fig. 1A. Positive selection of the B1-8 ^{hi} CFP$^+$ *Ly75*$^{+/+}$ B cells was induced by injecting αDEC-OVA. When compared directly with *Ly75*$^{-/-}$ B cells presenting lower levels of pMHCII in the same GC, positively selected *Ly75*$^{+/+}$ B cells interacted for a longer time with T_{FH} cells ($P < 0.0001$) (Fig. 2, A and B, and movie S5) and formed a greater number of stable contacts (> 5 min) (Fig. 2C). However, selection of *Ly75*$^{+/+}$ GC B cells did not alter the behavior of non selected *Ly75*$^{-/-}$ cells, which showed no significant change in contact duration or in the total number of interactions (> 0.5 min) with T_{FH} cells (Figs. 1D and 2, B and C, and movie S5). The majority of T_{FH} cells interacting with selected cells concurrently formed transient contacts with nonselected B cells (Fig. 2A and movie S5). We conclude that the increase in contact duration of T_{FH} cells with selected B cells does not substantially affect their interactions with nonselected B cells.

Our experiments indicate that increased contact size and duration correlates with the amount of pMHCII presented by GC B cells and their subsequent clonal expansion in the DZ (6), yet how these interactions affect T_{FH} T cell receptor (TCR) signaling is unknown. To examine the relationship between T-B contacts, TCR signaling, and B cell selection in the GC, we sought to measure intracellular Ca^{2+} levels in TFH cells. Traditional Ca^{2+} dyes cannot be used for this purpose because T cells divide extensively and dilute such tracers before reaching the GC (17). To circumvent this issue, we used mice expressing a genetically encoded Ca^{2+} indicator (GCaMP3), which changes its fluorescence intensity according to intracellular Ca^{2+} levels (18, 19). Lymphocytes from these mice showed an increase in intracellular fluorescence when stimulated with a Ca^{2+} ionophore or when stimulated through their antigen receptor (fig. S3 and movie S6).

Changes in Ca^{2+} fluorescence are best measured by comparison with a second dye that is insensitive to changes in intracellular Ca^{2+} levels. We therefore induced and imaged GCs, as described in Fig. 1A, using OT-II GCaMP3$^+$ DsRed$^+$ T cells and measured the ratio of GCaMP3:DsRed fluorescence intensity (fig. S4). To determine whether T_{FH} cell Ca^{2+} content is associated with changes in cellular dynamics, velocities at successive time points were measured (instantaneous velocity) and correlated with intracellular Ca^{2+} content (17). Under steady-state conditions, spikes in Ca^{2+} content in GC T_{FH} cells were rare (Fig. 3, A to C; fig. S5A; and movie S7). In contrast, αDEC-OVA injection increased the proportion of GC T_{FH} cells with GCaMP3:DsRed ratios above 0.05 from 9 to 68% (Fig. 3, A to C, and movie S7) and the average ratio by 8.3-fold (fig. S5A). Single T_{FH} cells that were actively engaged in B cell selection showed sustained increases in intracellular Ca^{2+} over time, which did not drop to control levels during the observation period (Fig. 3B). In addition, single T_{FH} cells also displayed frequent Ca^{2+} spike transients (Fig. 3, B and D). Both sustained and transient increases in T_{FH} intracellular Ca^{2+} levels were a result of TCR:pMHCII interactions (Fig. 3, B to D, and fig. S5A). We conclude that selection is associated with TCR:pMHCII–dependent increases in T_{FH} cell Ca^{2+} content that were both transient and long-term.

Increases in intracellular Ca^{2+} content in naïve T cells result in motility arrest and enhanced effector functions (17, 20, 21). By correlating intracellular Ca^{2+} content and instantaneous

velocity in unperturbed GCs, we found that T_{FH} cells moved at an average speed of 8.76 μm/min regardless of their Ca^{2+} content (Fig. 3C and fig. S5B). Consistently, in αDEC-OVA-targeted GCs the velocity of T_{FH} cells with high- and low- Ca^{2+} content was decreased to an average of 6.24 μm/min, and few, if any, of the actively engaged T_{FH} cells stopped moving or lost their morphological polarity while signaling (Fig. 3C, fig. S5B, and movies S7 to S9). However, there was no clear correlation between the level of Ca^{2+} increase and cell motility because both T_{FH} cells with high- and low- Ca^{2+} content had the same average velocity (Fig. 3C, fig. S5B, and movie S7). Nevertheless, by synchronizing transient small Ca^{2+} peaks of several T_{FH} cells, we found that these were precisely associated with a reduction in instantaneous velocity of ~2.5 μm/min (Fig. 3E, fig. S6, and movie S10).

Given these broad changes in Ca^{2+} content and the regulated T-B interactions, we sought to examine T_{FH} intracellular Ca^{2+} levels during the formation of T-B contacts. To this end, we imaged selection in GCs containing a 95:5 mixture of B1-8hi nonfluorescent *Ly75*$^{-/-}$ B cells, tdTomato^{+} *Ly75*$^{+/+}$ B cells, and OT-II GCaMP3^{+} T cells. Injection of αDEC-OVA induced the formation of T cell contacts with *Ly75*$^{+/+}$ B cells that were associated with transient spikes in T_{FH} intracellular Ca^{2+} content (Fig. 3, F and G, and movies S11 and S12). To determine whether these Ca^{2+} transients take place preferentially during T-B conjugate formation, we synchronized clearly isolated contact events and measured the average GCaMP3 fluorescence intensity in T_{FH} cells before and during these interactions. Although the intracellular Ca^{2+} levels in T_{FH} cells were high in αDEC-OVA–targeted GCs (Fig. 3B), an additional small increase at the onset of contact with selected B cells was detected (Fig. 3H and movie S10).

Changes in intracellular Ca^{2+} concentration control T cell effector functions, including the expression of IL-4 and IL-21 (20, 22), both of which are required for effective B cell immune responses (23). T effector cells can express either or both of these cytokines, and this multifunctionality is associated with enhanced immunity and vaccine responses (24–28). To determine whether the long-term increase in T_{FH} intracellular Ca^{2+} levels alters the quality of GC T_{FH} cells, we examined T cells derived from IL4/IL21 double reporter mice expressing *Il4-IRES-GFP* (29) and *Il21-IRES-Katushka* (fig. S7). Polyclonal OVA primed CD4^{+} T cells isolated from these mice were adoptively transferred into TCRβ-deficient mice along with B1-8^{hi} *Ly75*$^{+/+}$ and *Ly75*$^{-/-}$ B cells at a 5:95 ratio. Recipients were boosted with NP-OVA and injected 7 days later with either αDEC-CS or αDEC-OVA so as to induce selection. TFH cells were examined for cytokine expression 9 hours later by means of flow cytometry. αDEC-OVA injection resulted in a significant decrease in IL-4–IL-21–T_{FH} cells and a concomitant increase in IL-4^{+}IL-21^{+} multifunctional T_{FH} cells in the absence of cell division or a significant change in the number of single-cytokine-producing cells (Fig. 4, A and B, and fig. S8). Moreover, there was also a small but significant increase in the amount of IL-21, but not IL-4, produced by the double-positive cells, as measured by an increase in the mean fluorescence intensity of the reporters (Fig. 4, C and D). Thus, increased T_{FH} Ca^{2+} signaling during B cell selection is associated with a rapid change in the quality of the GC T_{FH} response, with increased development of multifunctional T_{FH} cells producing Ca^{2+}–dependent cytokines.

Our results demonstrate that T_{FH} cells respond to pMHCII on GC B cells during selection differently than the prolonged interactions of T cells with dendritic cells (DCs) in the T zone or with B cells at the T-B border (30–36). The transient interactional dynamics of T_{FH} cells in GCs allow them to continuously seek and find B cells presenting high levels of pMHCII and provide them with preferential help while permitting competitive opportunities for other GC B cells. This mode of B cell scanning allows T_{FH} cells to interact with many cells presenting a range of pMHCII levels, rather than forming a prolonged contact with a single high-affinity B cell.

Our experiments show that the increased size and duration of contacts between GC T_{FH} and selected B cells prolongs Ca^{2+} signaling and modifies the quality of the GC T_{FH} response. These events induce coexpression of the Ca^{2+}-dependent cytokines IL-4 and IL-21, which endow T_{FH} cells with effector capabilities that facilitate high affinity B cell selection.

Supplementary Material

Refer to Web version on PubMed Central for supplementary material.

Acknowledgments

We thank Dr. G. Victora for helpful discussions and suggestions and D. Bosque and T. Eisenreich for help with mouse colony management; A. Abadir for protein production; K. Yao for technical help. The data reported in this manuscript are tabulated in the main paper and in the supplementary materials. Z.S. is a Human Frontiers of Science Program fellow (reference #LT000340/2011-L). A.D.G is supported by NIH Medical Scientist Training Program grant T32GM07739 to the Weill Cornell/Rockefeller/Sloan-Kettering Tri-Institutional MD-PhD Program. Support for the Rockefeller University multiphoton microscope was granted by the Empire State Stem Cell Fund through New York State Department of Health contract C023046. Supported by NIH grants AI037526-19, AI072529-06, and AI100663-02 (M.C.N.), AR40072-24, and AR053495-08, and the Alliance for Lupus Research (J.E.C.). M.C.N. and R.A.F. are HHMI investigators.

References

1. Berek C, Berger A, Apel M. Maturation of the immune response in germinal centers. Cell. Dec 20.1991 67:1121. [PubMed: 1760840]
2. Allen CD, Okada T, Cyster JG. Germinal-center organization and cellular dynamics. Immunity. Aug.2007 27:190. [PubMed: 17723214]
3. Victora GD, Nussenzweig MC. Germinal centers. Annual review of immunology. 2012; 30:429.
4. Oprea M, Perelson AS. Somatic mutation leads to efficient affinity maturation when centrocytes recycle back to centroblasts. Journal of immunology. Jun 1.1997 158:5155.
5. Victora GD, et al. Germinal center dynamics revealed by multiphoton microscopy with a photoactivatable fluorescent reporter. Cell. Nov 12.2010 143:592. [PubMed: 21074050]
6. Gitlin AD, Shulman Z, Nussenzweig MC. Clonal selection in the germinal centre by regulated proliferation and hypermutation. Nature. May 29.2014 509:637. [PubMed: 24805232]
7. Crotty S. Follicular helper CD4 T cells (TFH). Annual review of immunology. 2011; 29:621.
8. Vinuesa CG, Cyster JG. How T cells earn the follicular rite of passage. Immunity. Nov 23.2011 35:671. [PubMed: 22118524]
9. Allen CD, Okada T, Tang HL, Cyster JG. Imaging of germinal center selection events during affinity maturation. Science. Jan 26.2007 315:528. [PubMed: 17185562]
10. Shih TA, Roederer M, Nussenzweig MC. Role of antigen receptor affinity in T cell-independent antibody responses in vivo. Nature immunology. Apr.2002 3:399. [PubMed: 11896394]
11. Schwickert TA, et al. In vivo imaging of germinal centres reveals a dynamic open structure. Nature. Mar 1.2007 446:83. [PubMed: 17268470]

12. personal communication.
13. Hauser AE, et al. Definition of germinal-center B cell migration in vivo reveals predominant intrazonal circulation patterns. Immunity. May.2007 26:655. [PubMed: 17509908]
14. Kitano M, et al. Bcl6 protein expression shapes pre-germinal center B cell dynamics and follicular helper T cell heterogeneity. Immunity. Jun 24.2011 34:961. [PubMed: 21636294]
15. Kerfoot SM, et al. Germinal center B cell and T follicular helper cell development initiates in the interfollicular zone. Immunity. Jun 24.2011 34:947. [PubMed: 21636295]
16. Shulman Z, et al. T follicular helper cell dynamics in germinal centers. Science. Aug 9.2013 341:673. [PubMed: 23887872]
17. Wei SH, et al. Ca2+ signals in CD4+ T cells during early contacts with antigen-bearing dendritic cells in lymph node. Journal of immunology. Aug 1.2007 179:1586.
18. Nakai J, Ohkura M, Imoto K. A high signal-to-noise Ca(2+) probe composed of a single green fluorescent protein. Nature biotechnology. Feb.2001 19:137.
19. Zariwala HA, et al. A Cre-dependent GCaMP3 reporter mouse for neuronal imaging in vivo. The Journal of neuroscience : the official journal of the Society for Neuroscience. Feb 29.2012 32:3131. [PubMed: 22378886]
20. Agarwal S, Avni O, Rao A. Cell-type-restricted binding of the transcription factor NFAT to a distal IL-4 enhancer in vivo. Immunity. Jun.2000 12:643. [PubMed: 10894164]
21. Negulescu PA, Krasieva TB, Khan A, Kerschbaum HH, Cahalan MD. Polarity of T cell shape, motility, and sensitivity to antigen. Immunity. May.1996 4:421. [PubMed: 8630728]
22. Kim HP, Korn LL, Gamero AM, Leonard WJ. Calcium-dependent activation of interleukin-21 gene expression in T cells. The Journal of biological chemistry. Jul 1.2005 280:25291. [PubMed: 15879595]
23. Ozaki K, et al. A critical role for IL-21 in regulating immunoglobulin production. Science. Nov 22.2002 298:1630. [PubMed: 12446913]
24. Betts MR, et al. HIV nonprogressors preferentially maintain highly functional HIV-specific CD8+ T cells. Blood. Jun 15.2006 107:4781. [PubMed: 16467198]
25. Newell EW, Sigal N, Bendall SC, Nolan GP, Davis MM. Cytometry by time-of-flight shows combinatorial cytokine expression and virus-specific cell niches within a continuum of CD8+ T cell phenotypes. Immunity. Jan 27.2012 36:142. [PubMed: 22265676]
26. Darrah PA, et al. Multifunctional TH1 cells define a correlate of vaccine-mediated protection against Leishmania major. Nature medicine. Jul.2007 13:843.
27. Kroenke MA, et al. Bcl6 and Maf cooperate to instruct human follicular helper CD4 T cell differentiation. Journal of immunology. Apr 15.2012 188:3734.
28. Luthje K, et al. The development and fate of follicular helper T cells defined by an IL-21 reporter mouse. Nature immunology. May.2012 13:491. [PubMed: 22466669]
29. Mohrs M, Shinkai K, Mohrs K, Locksley RM. Analysis of type 2 immunity in vivo with a bicistronic IL-4 reporter. Immunity. Aug.2001 15:303. [PubMed: 11520464]
30. Mempel TR, Henrickson SE, Von Andrian UH. T-cell priming by dendritic cells in lymph nodes occurs in three distinct phases. Nature. Jan 8.2004 427:154. [PubMed: 14712275]
31. Shakhar G, et al. Stable T cell-dendritic cell interactions precede the development of both tolerance and immunity in vivo. Nature immunology. Jul.2005 6:707. [PubMed: 15924144]
32. Miller MJ, Wei SH, Parker I, Cahalan MD. Two-photon imaging of lymphocyte motility and antigen response in intact lymph node. Science. Jun 7.2002 296:1869. [PubMed: 12016203]
33. Skokos D, et al. Peptide-MHC potency governs dynamic interactions between T cells and dendritic cells in lymph nodes. Nature immunology. Aug.2007 8:835. [PubMed: 17632517]
34. Okada T, et al. Antigen-engaged B cells undergo chemotaxis toward the T zone and form motile conjugates with helper T cells. PLoS biology. Jun.2005 3:e150. [PubMed: 15857154]
35. Qi H, Cannons JL, Klauschen F, Schwartzberg PL, Germain RN. SAP-controlled T-B cell interactions underlie germinal centre formation. Nature. Oct 9.2008 455:764. [PubMed: 18843362]
36. Schwickert TA, et al. A dynamic T cell-limited checkpoint regulates affinity-dependent B cell entry into the germinal center. The Journal of experimental medicine. Jun 6.2011 208:1243. [PubMed: 21576382]

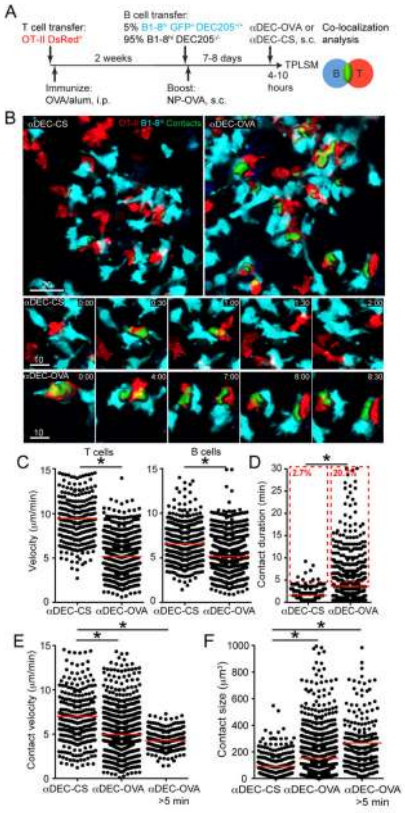

Fig. 1. Dynamics of T_{FH} and B cell interactions in the GC

(**A**) Timeline of the experimental protocol. i.p., intraperitonealy; s.c., subcutaneously. (**B**) GCs containing a 5:95 mixture of B1-8^{hi} *Ly75*$^{+/+}$ GFP^{+} B cells (cyan), B1-8^{hi} *Ly75*$^{-/-}$ B cells (non-fluorescent) and OT-II DsRed^{+} T cells (red) were imaged by TPSLM after s.c. injection of αDEC-OVA or αDEC-CS as control. T-B contacts (green) were detected by red and green pixel co-localization. Collapsed z-stacks of 40 μm depth (in 5μm steps) are shown. Bottom panels depict T and B cell dynamics over time. Images correspond to movies S1–3. (**C**) Velocity analysis of OT-II T cells and B1-8^{hi} B cells in GCs. (**D**) T-B contact duration as measured by the lifetime of the T-B co-localized areas. Percentages indicate events lasting > 5 min, marked by dashed red box. (**E**) T-B conjugate velocity was measured as the velocity of the T-B co-localized area. (**F**) Contact size analysis as measured by T-B co-localized area. Each data point represents a single cell and red lines represent mean values. Data in C-F were pooled from 2-4 mice imaged in 2-4 independent experiments. * $p < 0.0001$; two-tailed Student's *t*-test.

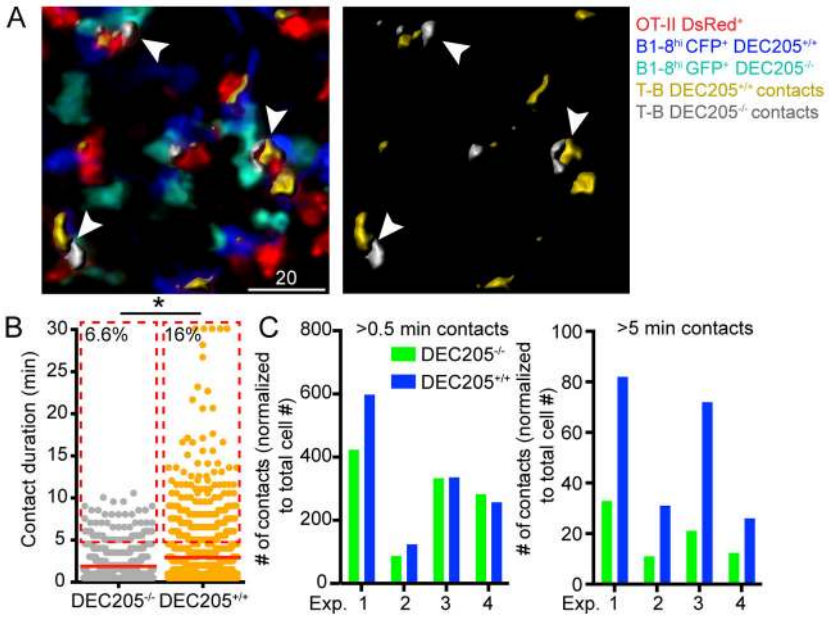

Fig. 2. T_{FH} cell interactions with selected and non-selected GC B cells

(**A**) GCs containing a ~5:5:90 mixture of B1-8^{hi} *Ly75*$^{+/+}$ CFP^{+} B cells (blue), B1-8^{hi} *Ly75*$^{-/-}$ GFP^{+} (green), *Ly75*$^{-/-}$ non-fluorescent B cells and OT-II DsRed^{+} T cells (red) were imaged by TPSLM after s.c. injection of αDEC-OVA. Contacts between OT-II T cells and either B1-8^{hi} *Ly75*$^{+/+}$ or *Ly75*$^{-/-}$ B cells are shown in yellow and grey, respectively. 40 μm deep, collapsed z-stacks (5 μm steps) are shown. Arrowheads indicate B1-8^{hi} *Ly75*$^{+/+}$ and *Ly75*$^{-/-}$ GC B cells interacting simultaneously with one OT-II T cell. (**B**) Quantitation of contact duration between OT-II T cells and B1-8^{hi} *Ly75*$^{+/+}$ or *Ly75*$^{-/-}$ B cells. Each data point represents a single cell and red lines represent mean values. Percentages indicate events > 5 min, marked by dashed red box. (**C**) The number of B cell contacts (> 0.5 min, left and > 5 min, right) with OT-II T cells was normalized to the number of B cells in each group. Exp., experiment. Data in B-C were pooled from 4 independent experiments. * $p < 0.0001$; two-tailed Student's *t*-test.

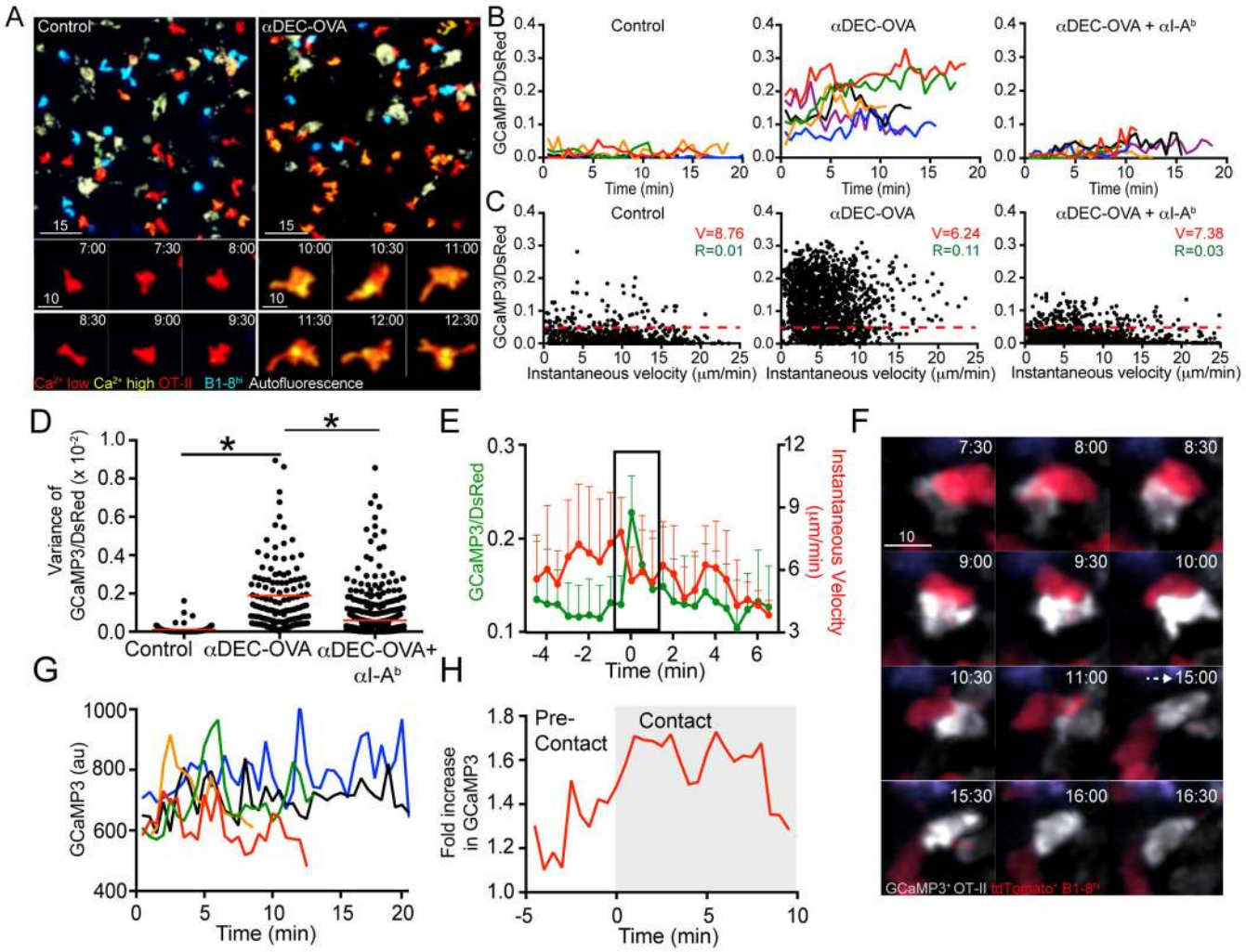

Fig. 3. T_{FH} cell Ca^{2+} signaling during B cell selection

(**A**) GCs containing a 5:95 mixture of B1-8^{hi} *Ly75*$^{+/+}$ CFP^{+} B cells (cyan), B1-8^{hi} *Ly75*$^{-/-}$ B cells (non-fluorescent) and OT-II DsRed^{+} GCaMP3^{+} T cells (red, Ca^{2+} low; yellow, Ca^{2+} high) were imaged by TPLSM in untreated mice or after s.c. injection of αDEC-OVA. The bottom panels depict dynamic changes in GCaMP3 fluorescence in individual OT-II T cells over time. (**B**) Traces show changes in the GCaMP3/DsRed ratios over time for 6 single T cells in each condition.αI-A^{b} was injected intravenously after αDEC-OVA injection. (**C**) Scatter plots depict the GCaMP3/DsRed ratio versus instantaneous velocity as measured at successive 30 sec intervals. Each dot represents a single cell at a single time point. Average velocity (V) and GCaMP3/DsRed ratios (R) of 2-3 experiments are indicated in red and green, respectively. (**D**) GCaMP3/DsRed ratio fluctuations in single cells (expressed as variance) under control and αDEC-OVA conditions. (**E**) GCaMP3/DsRed spikes of 9 cells were synchronized. Traces of GCaMP3/DsRed ratios average and corresponding instantaneous velocities are shown. The synchronized spikes fall in the black rectangle. Error bars, SEM. (**F**) OT-II GCaMP3^{+} T cells and B1-8^{hi} *Ly75*$^{+/+}$ tdTomato^{+} B cells were imaged in GCs over time as in A. Images correspond to movie S11. (**G**) Traces show GCaMP3 mean fluorescence intensities for 5 OT-II T cells in contact with B1-8^{hi} *Ly75*$^{+/+}$

tdTomato^{+} GC B cells. (**H**) Initiation of contacts were synchronized in 4 OT-II GCaMP3^{+} T cells and the corresponding average of GCaMP3 fluorescence intensity was traced before and during the contact (au, arbitrary units). Data is representative of 2–3 mice imaged in 2–3 independent experiments. * $p < 0.0001$; two-tailed Student's *t*-test.

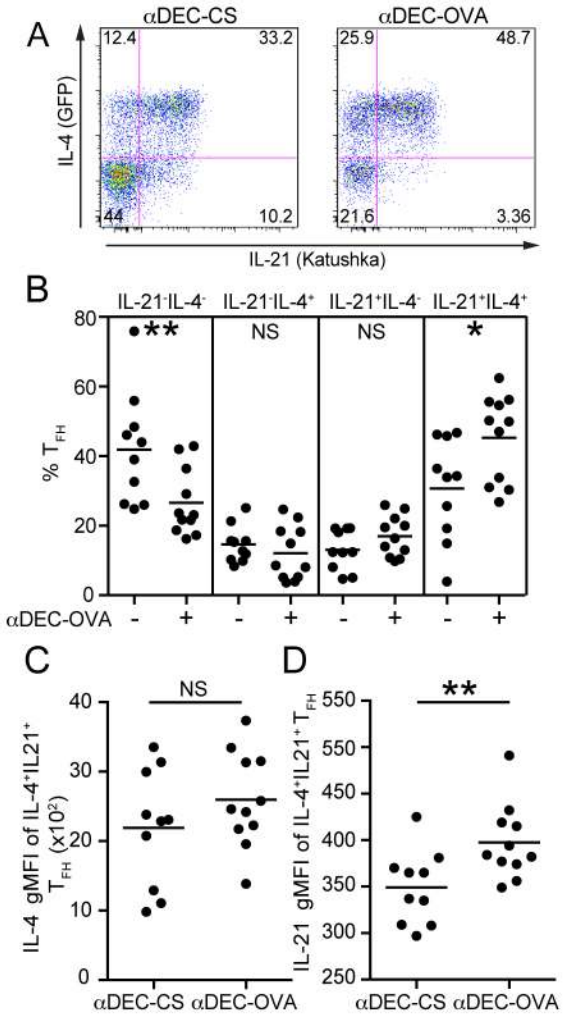

Fig. 4. Multifunctional T_{FH} cells during B cell selection

(**A-B**) $CD4^+$ T cells derived from OVA immunized *Il4-IRES-GFP* and *Il21-IRES-Katushka* double knock-in mice and a 5:95 ratio of B1-8^{hi} *Ly75*$^{+/+}$ and *Ly75*$^{-/-}$ B cells were transferred into TCRβ deficient mice, before boosting with NP-OVA. After 7 days, mice were injected with αDEC-CS or αDEC-OVA and lymph nodes were analyzed 9 hours later. The proportions of cytokine-expressing cells among T_{FH} ($CD8^-$, $B220^-$, $CD4^+$, $CD44^+$, $CD62L^-$, $CXCR5^{high}$ and PD-1^{high}) subsets are indicated. (**C-D**) gMFI of IL-4 (C) or IL-21 (D) reporter expression. Each data point represents a single mouse and lines represent mean values. Pooled data from 3 experiments each with 3–4 mice per condition. * p = 0.021; ** p = 0.014 ***; p = 0.012; two-tailed Student's *t*-test. NS, not significant.